5-2019

Magnetic Minerals of the Lower Poleslide Member of the Brule Formation, Badlands National Park

Rebecca V. Kipf

UNIVERSITY OF NORTHERN COLORADO
Greeley, Colorado
The Graduate School

MAGNETIC MINERALS OF THE LOWER POLESLIDE MEMBER OF THE BRULE FORMATION, BADLANDS NATIONAL PARK

A Thesis Submitted in Partial Fulfillment
of the Requirements for the Degree of
Master of Arts

Rebecca V. Kipf

College of Natural and Health Sciences
Department of Earth and Atmospheric Sciences

May 2019

This Thesis by: Rebecca V. Kipf

Entitled: *Magnetic Minerals of the Lower Poleslide Member of the Brule Formation, Badlands National Park*

has been approved as meeting the requirement for the Degree of Master of Arts in the College of Natural Health Sciences in Department of Earth and Atmospheric Sciences. Program of Earth Science.

Accepted by the Thesis Committee:

_____
Dr. Emmett Evanoff, PhD, Chair

_____
Dr. Graham Baird, PhD, Committee Member

_____
Byron Straw, MA, Committee Member

Accepted by the Graduate School

_____
Linda L. Black, Ed.D
Associate Provost and Dean
Graduate School and International Admissions
Research and Sponsored Projects

ABSTRACT

Kipf, Rebecca, V., *Magnetic Minerals of the Lower Brule Formation, Badlands National Park.* Unpublished Master of Arts Thesis, University of Northern Colorado, 2019.

The White River Group in Badlands National Park is significant because it contains abundant mammal fossils. Many of these fossils are unique to the Great Plains and one of the major challenges has been to learn where these fossils fit in the geologic global time scale. Paleomagnetic studies have been instrumental in correlating and dating these faunas. The purpose of this study is to look at the specific magnetic mineralogy for a complete stratigraphic column of the lower Poleslide Member of the Brule Formation at Cedar Pass. This study attempts to determine what minerals provide the paleomagnetic remanence in these rocks.

This study used three techniques to determine the quantities and kinds of magnetic minerals in the samples and determine if there are any significant patterns in the amounts of magnetic minerals or in the types of magnetic minerals. The magnetic minerals were removed from crushed rock samples with a strong bar magnet. Portions of the separated magnetic minerals were treated with hydrochloric acid (HCl), to separate the easily dissolved magnetite grains from other resistant magnetic materials. Four samples were analyzed with a scanning electron microscope to determine the composition of the magnetic minerals. These techniques were used to determine if there

are significant patterns in the amounts and kinds of magnetic materials through the stratigraphic section.

The overall quantities of magnetic minerals in the rock samples ranted from 0.05% to 0.63% of the total rock mass. The most significant results show that the quantities of HCl resistant minerals changes at 31.5 meters above the base of the stratigraphic section. Below this level, acid-resistant magnetic minerals occur in low concentrations in many of the treated samples. Above the 31.5 m level, these acid-resistant minerals are essentially absent, occurring in only trace amounts (<0.01% of the total rock mass). The SEM analysis is not conclusive in confidently identifying the specific minerals. However, the evidence suggests the magnetic minerals contain magnetite, titanomagnitite or hemo-ilmenite and perhaps ulvöspinel.

ACKNOWEDGEMENTS

This thesis was not completed without the help of a number of individuals. I would like to take a moment to thank them for their hard work, for their encouragement, and for their guidance both on this project and throughout my experiences at the University of Northern Colorado. Dr. Emmett Evanoff inspired me with a love for geology. He was an excellent example of hard work and knowledge. His enthusiasm fueled my own. Dr. Graham Baird was instrumental in helping me understand the mineralogy that made this project possible. He also challenged me to be a better geologist and to keep a high standard. He also believed that I could meet that high standard and was there when I needed his guidance and expertise. Byron Straw taught me how to do geologic research but he also has influenced my teaching career as I try to emulate his enthusiasm for teaching and care for his students.

I would also like to thank the other professors in the Earth and Atmospheric Science Department, particularly Dr. Cindy Shellito, Wendi Flynn, David Lerach. I had the opportunity to take their classes and work with them as a teaching assistant and they all supported me as a student and encouraged me as a teacher. I would also like to thank the chair of the department Dr. William Hoyt for his support and encouragement.

Lastly, I would like to thank Ann Dickinson for her friendship, encouragement, and support during this project and during my time at the University of Northern Colorado.

TABLE OF CONTENTS

LIST OF TABLES

LIST OF FIGURES

CHAPTER I

INTRODUCTION

Project Description

The sedimentary rocks of the badlands region are significant because of the early mammal fossils they contain. These fossils are rare and they provide information about the development of mammals. One of the main challenges has been to establish ages for rocks and fossils. The rock layers were initially identified based on the fossil assemblages that were formalized by Wood and others (1941). Paleomagnetic research has been another area of study that has the potential of connecting the badlands time scale to the global timescale (Prothero, 1985; Tedford and others, 1996; and Prothero and Whittlesey, 1998). As part of the paleomagnetic research, it is important to understand the magnetic minerals that are present and their distribution.

This project focuses on identifying and quantifying the magnetic minerals present in a complete stratigraphic column representing the lower Poleslide Member of the Brule Formation in Badlands National Park. It is set to answer several questions:

Q1 What are the magnetic minerals and quantities of magnetic minerals in the Cedar Pass Section?

Q2 Are there any specific patterns in the distribution of magnetic minerals in the section?

Stratigraphy of Badlands National Park Overview

The Badlands is a geographical area located in the southwest part of South Dakota known for its stunning collection of erosional geologic features. The area is marked by

cliffs, spires, buttes and valleys carved through distinct layers of sedimentary rock. The name badlands is a translation of the Lakota word Makosica, referring to the area being a bad land to traverse (Benton and others, 2015). Early explorers and trappers experienced difficulties in crossing these landforms, but they also discovered that the area was rich in vertebrate fossils.

The discovery of fossils is one of the key events that contributed to the formation of Badlands National Park. The first announcement to science of early mammal fossils from the Badlands was by Prout (1846). Subsequently, many geologists and naturalists came to the Badlands to collect and study the White River Formation fossils. In 1939, Badlands National Monument was established to protect the landforms and preserve the fossils (Benton and others, 2015). In 1978, the monument was expanded and became Badlands National Park. The current park consists of two sections, the North Unit and the South Unit, and covers about 244,000 acres (Stoffer, 2003). Figure 1 shows a map of Badlands National Park.

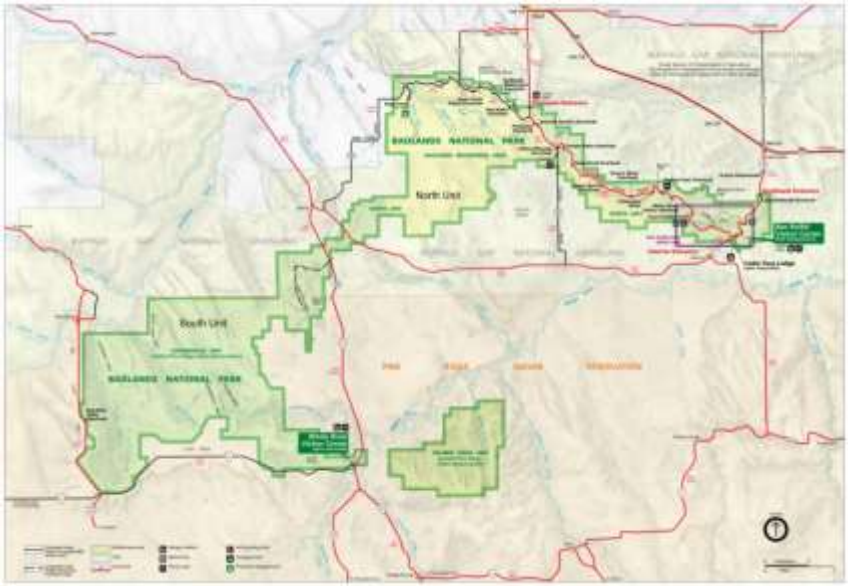

Figure 1. Map of Badlands National Park. Modified from (http://npmaps.com/wp-content/uploads/badlands-map.jpg, (Jan. 2019)) Outline is location of Figure 2.

There are six geologic formations exposed in Badlands National Park: the Pierre Shale, Fox Hills Formation, Chamberlain Pass Formation, Chadron Formation, Brule Formation, and Sharps Formation. The oldest formation is the Pierre Shale. The shales of this formation were deposited when the Western Interior Seaway covered the area. Marine fossils indicate a Late Cretaceous age and have an absolute age of approximately 70 Ma (Benton and others, 2015).

After the retreat of the Western Interior Seaway, there was a period of erosion creating an unconformity with a gap in time of about 30 million years. During this time, the Black Hills region was uplifted as part of the Laramide orogeny. In the Badlands, the surface remained horizontal, but the Pierre Shale was tilted and eroded in the Black Hills before further deposition (Benton and others, 2015). The sandstones and silty shales of the overlaying Fox Hills Formation were part of advancing river deltas into the Pierre seaway. This formation contains a mixture of both marine and terrestrial fossils and is dated at about 67 Ma (Benton and others, 2015).

The next three formations, the Chamberlain Pass Formation, Chadron Formation, and Brule Formation belong to the White River Group. The Chamberlain Pass Formation consists of red mudstone and lenticular white sandstone sheets that overlie paleosols. The age of this formation is late Eocene about 36.5 – 34 Ma and its fossils are part of the late Duchesnean or early Chadronian land mammal ages (Evans and Terry, 1994). The Chadron Formation consists of greenish gray claystone beds with lenticular and sheet sandstones. The age is late Eocene (Prothero and Emery, 2004). There are three members: the Ahern, Crazy Johnson, and Peanut Peak members (Clark, 1954). The

fossils of the Chadron Formation are characteristic of the Chadronian land mammal age (Wood and others, 1941; Benton and others, 2015).

The Brule Formation is of Oligocene age and lies on an erosion surface cut into the Chadron Formation (Evanoff and others, 2010). There are two members of the Brule Formation: the Scenic Member and the Poleslide Member. The Scenic Member has three subdivisions including a lower mudstone interval, a series of muddy sandstone blankets, and an upper mudstone interval. The Poleslide Member also has three subdivisions and consists of massive siltstone beds and widespread sandstones. The lower part of the Poleslide Member is discussed in this paper and has twelve distinct units. Where the study samples were collected, the lower Poleslide is capped by a marker layer that is referred to as the Cedar Pass white layer (Evanoff and others, 2010). The middle Poleslide Member consists of massive siltstones with globular carbonate nodules. The upper Poleslide Member has alternating thick sheets of siltstone and sandstone (Benton and others, 2015).

The Poleslide Member of the Brule Formation is separated from the overlying Sharps Formation by the Rockyford Ash. This layer is a volcanic tuff that has a distinct lower contact and a diffuse upper contact. It has abundant euhedral crystals of biotite and hornblende. It also has less abundant zircon, apatite, and clinopyroxene (Larson written comm., 1998). The Rockyford Ash occurs only on the west side of the North Unit in Badlands National Park. The Rockyford ash has not been dated. The minerals in the Cedar Pass white layer are much more weathered, have few euhedral biotite crystals and no hornblende crystals, and are consistent with the mineral composition of the surrounding siltstones of the lower Poleslide Member (Benton and others, 2015). The

Sharps Formation is characterized by massive, sandy siltstone beds. The fossils in this formation are from the Arikarean land mammal age (Tedford and others, 1996).

Location of the Study Section

The Cedar Pass section is located to the northeast of the Visitor Center Park Headquarters in the North Unit of Badlands National Park (Figure 1). Figure 2 and 3 show a detailed map of the location of the outcrops and sampled sections. The sections include three successive partial sections that were connected by individual laterally continuous layers. Figure 4 shows images of the sampled section outcrops

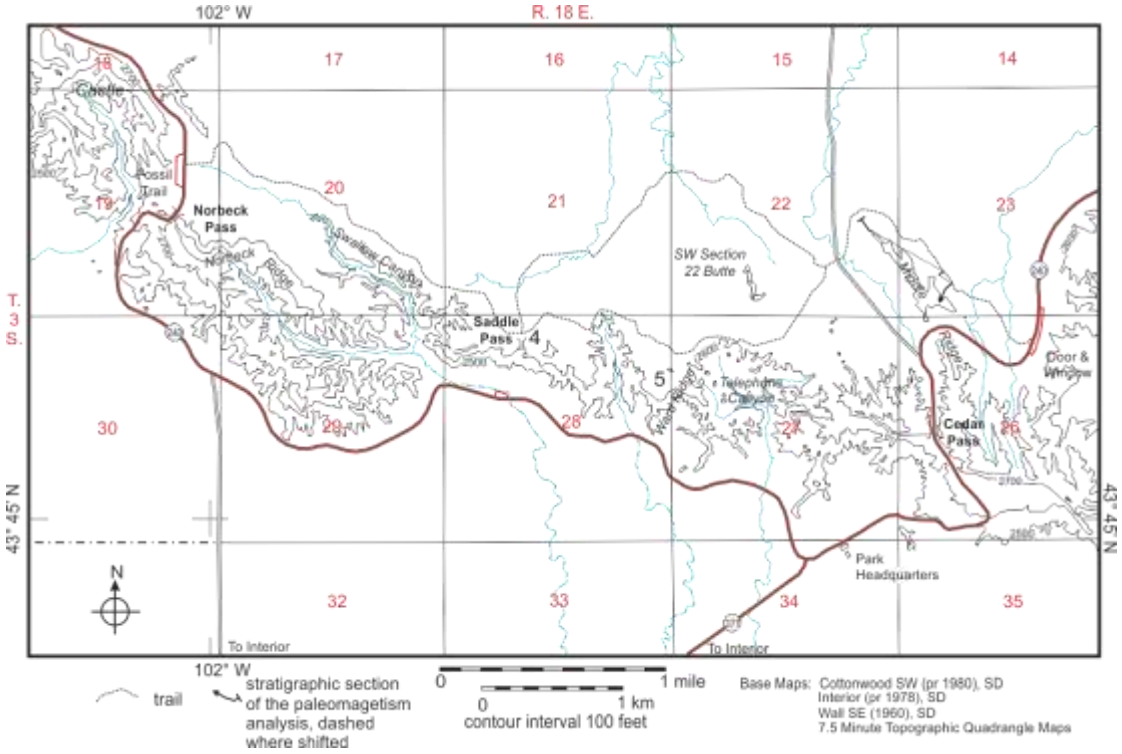

Figure 2. Index map of the eastern side of the North Unit of Badlands National Park showing the location of the stratigraphic section sampled for paleomagnetic analysis (small arrows in sections 22 and 23). Benton and others, 2009, Figure 3-1.

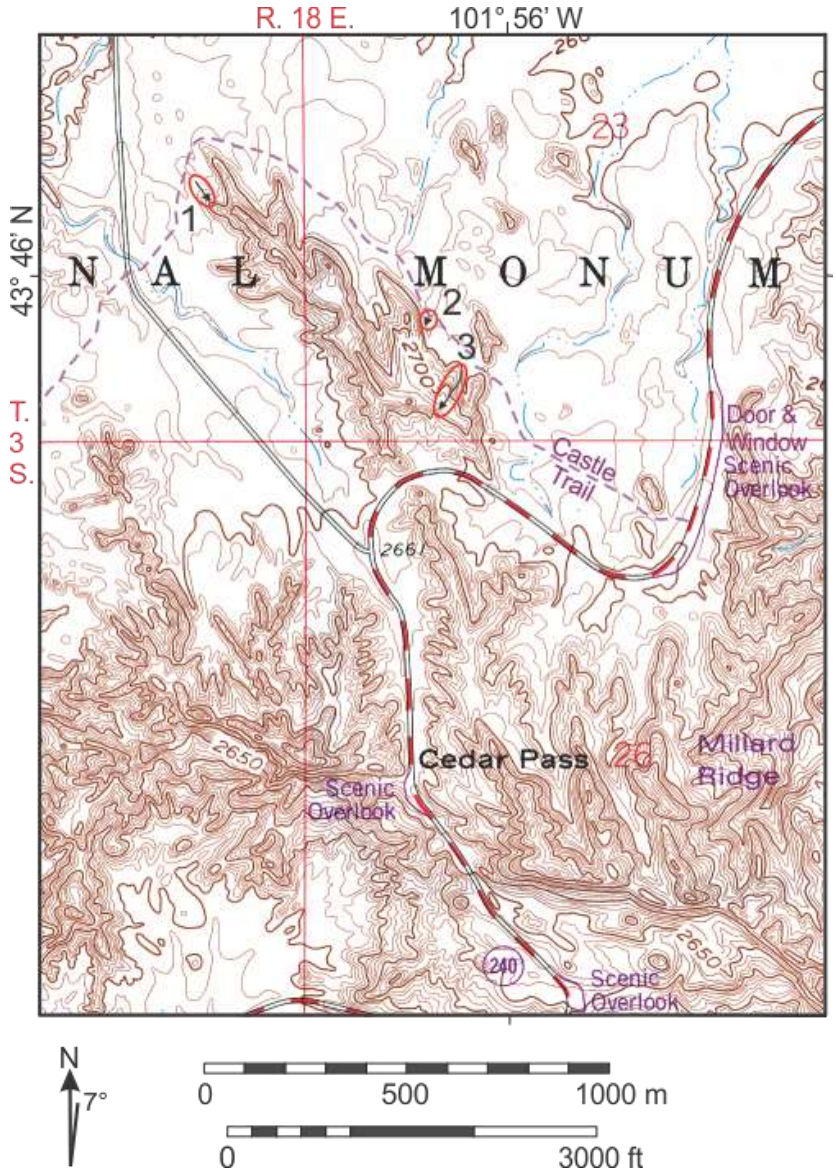

Figure 3. Detailed map of the stratigraphic sections used. (1) Tbp2 section where units 1-2 were sampled. (2) CPMS3 section where units 3-4c were sampled. (3) CPms4 section where units 4d through the Cedar Pass white layer were sampled. The base map is the Cottonwood SW, South Dakota, 7.5 minute topographic map (1960, photo revised 1980).

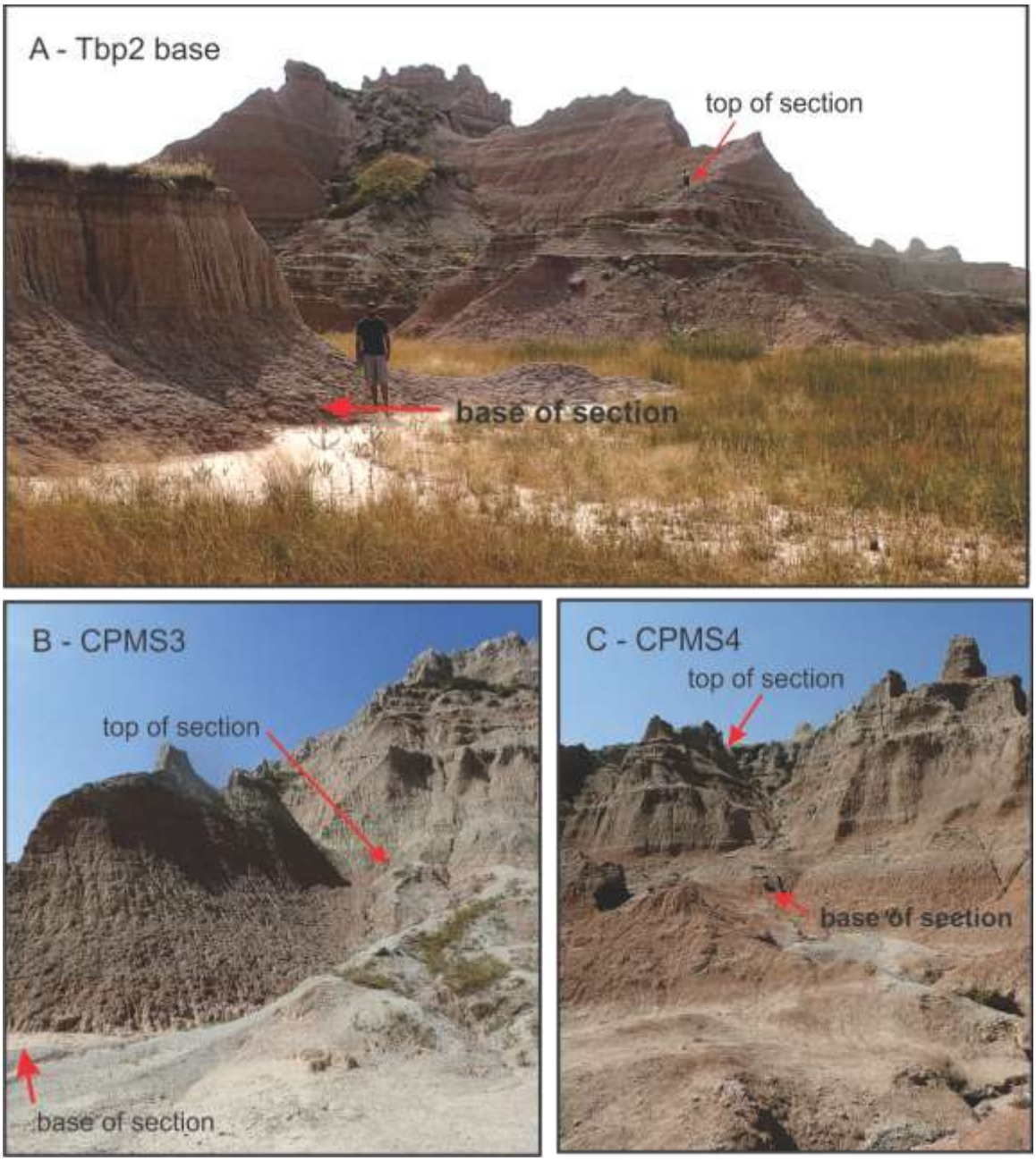

Figure 4. Localities of the stratigraphic sections sampled for paleomagnetism studies. A is the lower part of the Tbp2 section. The Tbp 2 section was measured and sampled from the foreground along the ridge to the top. B is the location of the CPMS3 section. Section was measured and sampled along the side of the gully. C is the location of the CPMS4 section. Section was measured from the bottom, along the sides of the steep gully behind the starting point, and ended on the Cedar Pass white layer at the top of the gully. Photographs by Evanoff, 2018.

Stratigraphic Units of the Lower Poleslide Sampled Section

Evanoff described the section used in this study, as part of the Poleslide Fossil Survey Project (Benton and others, 2009, hereafter referred to as the Poleslide Project). Figure 5 is a detailed stratigraphic column of the sampled section. The samples are labeled with a CP designating the site location and a number related to the stratigraphic position in the column.

There are twelve distinctive units in the lower Poleslide Member of the Brule Formation in the eastern half of the North Unit of Badlands National Park. The massive siltstone beds represent wind deposits. Volcanic ash from sources far to the west were reworked by the wind and redeposited as windblown dust or loess (Benton and others, 2015). The source of the volcanoclastic material was originally from the area that is now the Great Basin of Nevada and western Utah (Larson and Evanoff, 1998). Two of the units, unit 2 and unit 11 are mainly sandstone and they represent a fluvial depositional environment. The rivers were not laterally restricted in the area and resulted in broad sandstone deposits with alternating layers of sandstone, muddy sandstone, and mudstone (Benton and others, 2009).

Unit 1, at the base of the section, consists of massive siltstone beds with scattered globular carbonate-cemented nodules. The siltstone is light gray, weathers to a tan, and the nodules are a light tan (Benton and others, 2009). Unit 1includes samples CP1.5, CP3.0 and CP4.5.

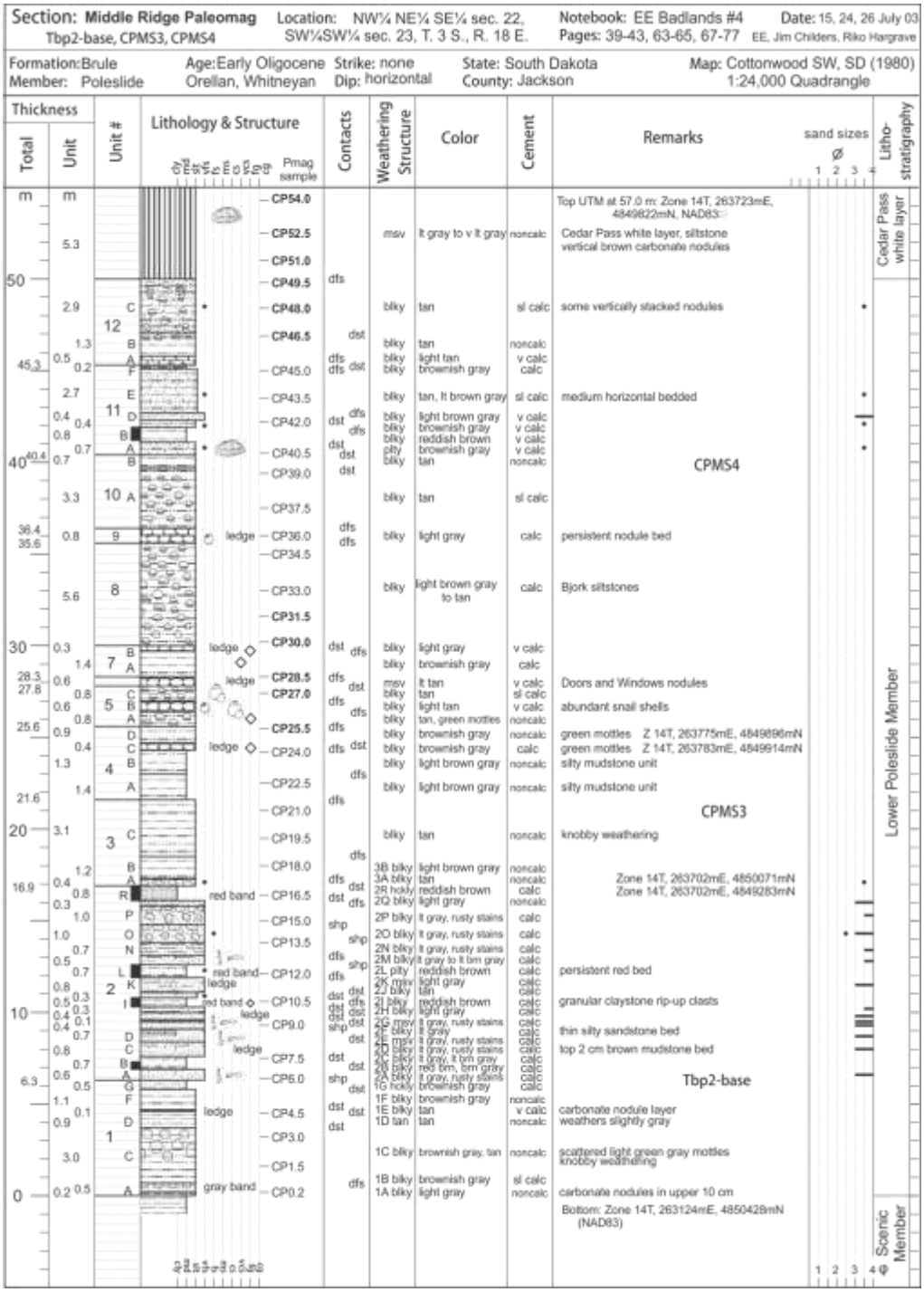

Figure 5. Graphic log of the Middle Ridge paleomag composite section at Cedar Pass as measured by Evanoff, Childers, and Hargrave in July 2003. The positions of the paleomagnetism rock samples used in this study are shown on the right side of the Lithology and Structure column. The paleomagnetic samples in bold are those with normal polarity. Unpublished diagram by Evanoff, 2018.

Unit 2 is the first of the two sandstone units in the section and is a sequence of alternating sandstone and muddy sandstones. The sandstones are typically light gray with beds of very fine to fine-grained sand. The beds can show horizontal bedding or be structureless. There are also brown to reddish brown mudstone and claystone beds that make up less than 25% of the unit. There are eight samples from this section beginning with CP6.0 and ending with CP16.5.

Unit 3 consists of tan, massive, siltstone beds. Carbonate nodules are scattered in the lower section of the unit but more abundant and often occur in discontinuous layers in the upper section (Benton and others, 2009). Samples CP18.0, CP19.5, and CP21.0 are representative of unit 3.

Unit 4 has two main divisions. The lower portion of the unit has brown silty mudstone beds. It typically has an indistinct contact with the upper brown siltstones. Lateral variations exist within this unit at other locations including a limestone bed near the Door and Window trail but are not found in this section (Benton and others, 2009). Samples CP22.5, CP24.0, and CP25.5 are from unit 4.

Unit 5 is a brownish gray, massive siltstone layer that weathers gray. In the Cedar Pass location, it has globular carbonate nodule layers. It is exposed in cliffs supported by the nodular layer of unit 6 (Benton and others, 2009). CP27.0 is from unit 5.

Unit 6 is a widespread carbonate nodule layer that is informally named the Door and Window nodular ledge. The nodules are light tan and interlock to form a carbonate cemented siltstone bed. Trace fossils such as vertical and horizontal tubes, rhizoliths, and siltstone spheres are common in this layer as well as shells of fossil land snails (Benton and others, 2009). CP28.5 is representative of this unit.

Unit 7 has a section with is a massive siltstone bed that grades upward to a nodule layer. The lower part is buff colored and the upper half is light gray. There are only rare fossils in this unit (Benton and others, 2009). There is no sample from this unit in this study.

Unit 8 has thick, massive, tan, siltstone beds with scattered globular carbonate nodules. In some locations the nodule are stacked vertically and represent carbonate accumulation around plant roots. This is a highly fossiliferous unit and is informally named the Bjork Siltstone beds for Dr. Philip Bjork who spent decades collecting fossils in the Cedar Pass area (Benton and others, 2009). Samples CP30.0, CP31.5, CP33.0, and CP34.5 are from unit 8.

Unit 9 is another widespread carbonate nodule layer that is light gray to light tan in color. The nodules form a well-cemented siltstone layer that is a widespread bench supporter (Benton and others, 2009). CP36.0 is part of this unit.

Unit 10 is massive, thick siltstone beds with scattered globular carbonate nodules and thin nodule layers. In some localities, the nodules in this layer are stacked. The unit is typically exposed in a cliff face below the sandstone ledges of unit 11 (Benton and others, 2009). Samples CP37.5 and CP39.0 are from unit 10.

Unit 11 is the second sandstone unit in the section. It is a sequence of sandstone and muddy sandstone sheets that range from brownish gray to reddish brown. Both are very fine-grained sands with a silty or muddy matrix. The thicker beds often show horizontal bedding with vertical and horizontal tubes that have a diameter of about 0.5 cm. The unit can also have thin claystone, mudstone, and siltstone beds (Benton and others, 2009). Samples CP40.5, CP42.0, CP43.5, and CP45.0 are from unit 11.

Unit 12 is thick, massive siltstone beds that are light gray to very light brownish gray. They contain globular carbonate nodules scattered throughout the unit with a layer of nodules occurring about 0.7 to 1.6 m above the base of the unit. Vertically stacked nodules are common in the upper siltstone bed of this unit (Benton and others, 2009). CP46.5, CP48.0, and CP49.5 are representative of unit 12.

The final set of samples at the top of the Cedar Pass section are from a bed informally called the Cedar Pass white layer (CPWL). This unit is composed of siltstones that are very light gray (near white) with brown vertically-elongated nodules. (Benton et. al., 2009). The samples from this bed include CP51.0, CP52.5, CP 54.0, and CP55.0.

CHAPTER II

PREVIOUS STUDIES

Faunal Dating

One of the biggest challenges in the study of the White River Group has been dating the rocks and faunas. Early geologists named the various stratigraphic subdivision based on the prominent fossils found within the units. The lower Poleslide Member of the Brule Formation was known as the top of the turtle/Oreodon beds, and the lower *Protoceras/Leptauchenia* beds (Wanless, 1923). These faunal subdivisions were formalized into the North American land mammal ages by Wood and others (1941). The boundary between the Orellan and Whitneyan land mammal ages falls within the lower Poleslide Member at the base of unit 8 (Evanoff and others, 2010). These developments over time have been important, but have not solved the challenge of connecting the White River fauna to the global time scale. For example, the original age determination for the Chadronian, Orellan, and Whitneyan land mammal ages were thought to be Oligocene (Osborn and Matthew, 1909; Wood and others, 1941). However, radiometric dating of tuffs in the White River sequence now indicates Charonian faunas are late Eocene in age, and Orellan and Whitneyan faunas are early Oligocene in age (Prothero and Emery, 2004).

Dating by Paleomagnetic Analysis

Paleomagnetic data is an important tool in determining the relative age of sedimentary rock. Magnetic minerals such as magnetite are common in small quantities

in most rocks. The magnetic signature carried by these minerals can be used to determine the Earth's magnetic polarity at the time of formation. With improved technology, it has become possible to determine the strength and direction of the magnetic signals preserved in sedimentary rocks, which contain only trace amounts of magnetic minerals (Tarling, 1999).

Prothero and others (1983) was the first magnetiostratigraphic studies completed for the White River Group across Wyoming and Nebraska. Eighteen localities were sampled including one in the Cedar Pass area. Based on the paleomagnetic data, they determined that the magnetic remanence was carried by magnetite or titanomagnetite. They also believed that goethite was present (Prothero and others, 1983). In the Flagstaff Rim section in Wyoming, there were four ash deposits that were radiometrically dated and were used to correlate the paleomagnetic data with the global magnetic polarity time scale. They assigned an age of approximately 30.7-32.4 Ma for the fauna of the Orellan land mammal age (Prothero and others, 1983).

Prothero and Whittlesey (1998) used paleomagnetic data to more accurately date the Orellan and Whitneyan land-mammal ages. In the analysis of additional samples, including in the Cedar Pass area, they determined that the primary carrier of magnetic remanence was magnetite but in several samples, they found that hematite or goethite was more important. They determined that the date of the Chadronian-Orellan Boundary is 33.7 Ma. The Orellan-Whitneyan boundary is 32.0-31.4 Ma and the Whitneyan-Arikareean boundary is at 30.0 Ma (Prothero and Whittlesey, 1998).

CHAPTER III

METHODS

Field Sampling

Dr. Emmett Evanoff, Jim Childers, and Riko Hargrave collected the samples during the summer of 2003. Three outcrops were described and sampled to create a complete composite section of the lower Poleslide member of the Brule Formation. The section was measured using a Jacob's staff and Abney level. Plastic sleeved nails were driven into the rock in 1.5-meter intervals and the section was described in detail using the markers as thickness controls. Rock samples ranging in size from 1-3 cubic decimeters were collected at the markers. While still attached to the outcrop each sample was marked with a horizontal line and a true north arrow based on a 7˚E declination. The samples were removed from the outcrop and labelled directly on the rock by its field number consisting of CP for Cedar Pass and its stratigraphic position. Each sample was wrapped in newspaper and secured with masking tape that was also labeled with the field number. Three, 8 cm^3 cubes were cut from each sample parallel to the N-S, E-W, and top and bottom faces and the top was marked with a north arrow. Each cube was also marked with the field number. The samples were used for paleomagnetic analysis. The remaining rock materials from the samples were used for this project.

Method of Magnetic Separation

A total of 300 grams of each sample was processed. In order to be efficient, each sample was divided in half and processed separately. Approximately 150 grams of rock were pulverized using a mortar and pestle. The powder was mixed with tap water in a 500 ml beaker to produce sediment slurry. A strong bar magnet was placed in a plastic bag and was used to remove the magnetic minerals that were placed in a small ceramic dish. Figure 6 shows the setup for the separation process. The magnetic portion was dried in an oven at 100˚ F for 24 hours. The bar magnet was used to perform a dry separation to remove more of the remaining clay. Figure 7 shows how the dry separation was accomplished and Table 1 lists the procedures followed.

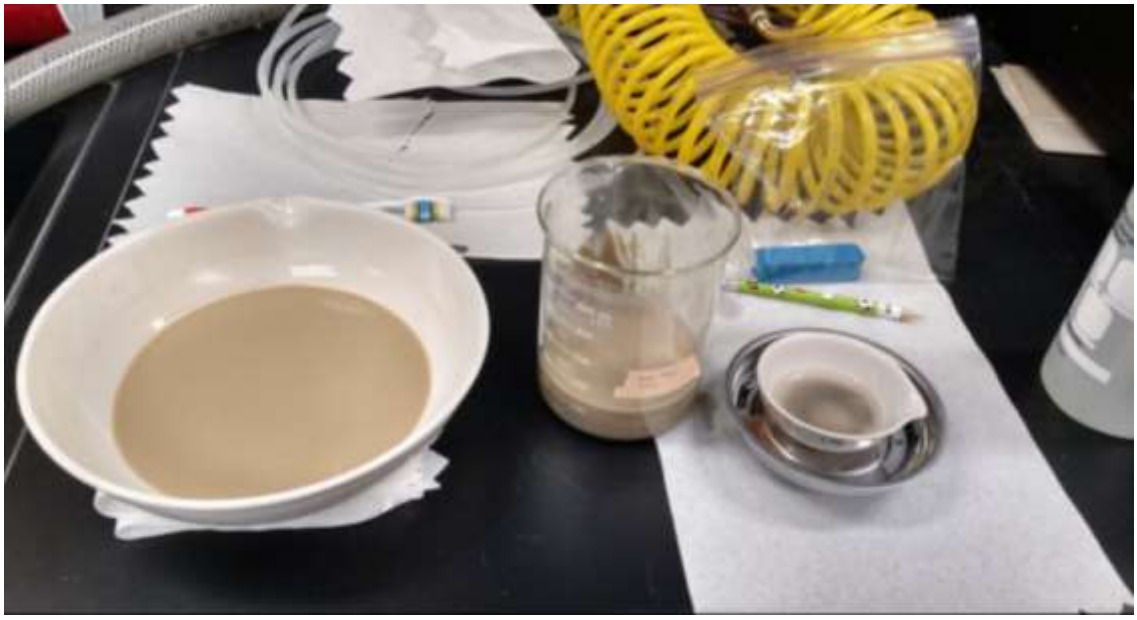

Figure. 6. Set up for magnetic separation process included a ceramic bowl for separation, beaker for creating slurry, strong bar magnet in plastic bag, and small ceramic dish for magnetic The ceramic dish is in a magnetic ash tray which was used to keep the dish from being knocked over.

Table 1. Steps for magnetic separation

Step	Action
1	Split the rock into two 150 g samples using the mortar and pestle to break the rock if needed.
2	Pulverize one 150 g sample to a fine powder using the mortar and pestle.
3	Record the mass of the powder.
4	Place the powder in a 500 ml beaker, fill to 500 ml with tap water and mix well with a non-metallic instrument.
5	Pour approximately 250 ml of the slurry into a low ceramic bowl.
6	Refill the 500 ml beaker with water and mix. Allow the slurry to settle during the completion of steps 7-12.
7	Place a bar magnet inside plastic bag.
8	Drag the magnet through the slurry in the bowl while rotating the bowl slowly.
9	At the end of the rotation or when necessary, hold the sandwich bag over the small ceramic dish, remove the magnet from the bag and with a gentle stream of water from a water bottle rinse the magnetic minerals into the small ceramic dish.
10	Mix the slurry in the ceramic bowl.
11	Repeat steps 7-10 until no additional magnetic material is collected.
12	Discard the slurry in the bowl.
13	Repeat steps 5-12 until the water in the 500 ml beaker is mostly clear.
14	Mix the slurry in the 500 ml beaker well and pour about half in the bowl. Do not add more water to the beaker.
15	Separate the magnetics in the same manner that was used before.
16	Repeat with the last half of the slurry. (The solid material from these last two separations were collected and dried for future projects)
17	Rinse the bowl and fill with approximately 200 ml of water.
18	Rinse the magnetic sample from the ceramic dish into the clean water.
19	Use the same method with the bar magnet to separate the magnetics. There will be a small amount of clay material in the bowl.
20	Discard the water. Any solid material was added to the non-magnetic material that was saved for future projects.
21	Use the bar magnet on the bottom of the ceramic dish to help hold the magnetic sample in place and pour off the excess water.
22	Place the ceramic dish holding the magnetic sample in the Napro 420 drying oven on setting 2 for 24 hours.

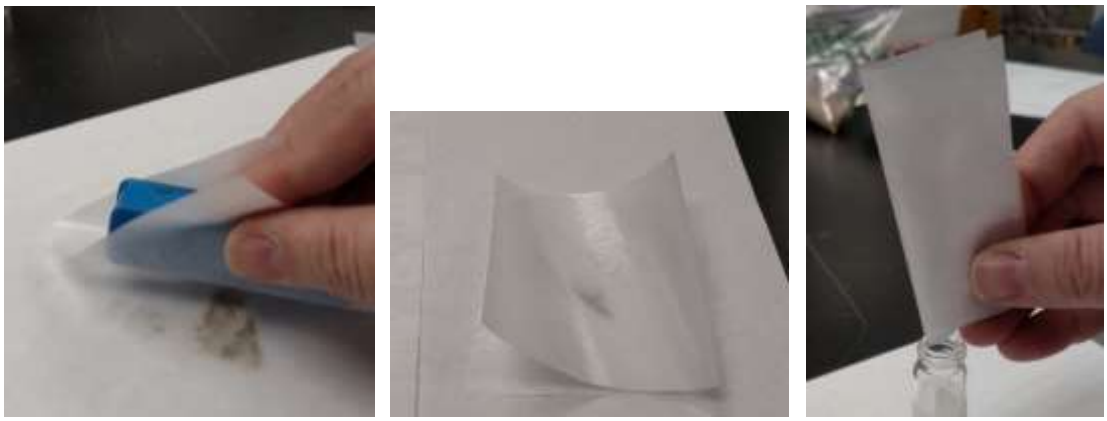

Figure 7. Images of dry separation process from left to right: Collecting magnetic material, magnet is removed leaving magnetic material on bottom sheet of weight paper, magnetic material is placed in a vial.

Hydrochloric Acid Separation

For each sample, 0.15 g of the magnetic mineral sample was placed in a small ceramic dish and placed in a fume hood. The material was covered with approximately 10 ml of 37% hydrochloric acid (HCl). If magnetite is present in the sample, the sample turns yellow as magnetite is dissolved by HCl. In a few samples, the color was more orange indicating the presence of hematite. After 24 hours, the sample was rinsed with a small amount of tap water to remove any residue from the HCl and allowed to dry. A mass was taken of the HCl sample in the dish and the sample was again covered with HCl. Figure 8 shows several samples in HCl. This process was repeated until there was no additional change in mass for three consecutive measurements. Table 2 gives the steps that were followed.

Figure 8. Samples in HCl in the fume hood.

Table 2. Steps to the HCl process

Step	Action
1	Record mass of labeled small ceramic dish.
2	Place 0.15 g of magnetic sample in the dish.
3	In the hood, add approximately 10 ml of 37% HCl.
4	Let sit for 24 hours.
5	Decant any remaining HCl onto limestone in disposal container and allow to dry.
6	Rinse sample with a small stream of tap water from water bottle. Pour liquid into disposal container.
7	Allow sample to dry.
8	Take a mass of the sample and record.
9	Return to hood and add approximately 10 ml of 37% HCl.
10	Repeat process until there is no change in mass for 3 consecutive readings.
11	Carefully remove remaining material using a piece of weigh paper.
12	Follow the instructions for doing a dry separation using a strong bar magnet outlined in the magnetic separation step.
13	Place magnetic material in a labeled glass vial.
14	Place non-magnetic in a separate labeled glass vial.

After the hydrochloric acid, a small quantity of fine clay particles remained. In order to insure that the mass was an accurate representation of the magnetic minerals, a final dry magnetic separation was performed in the same manner as in the magnetic separation step. A mass was recorded for both. The mass of the non-magnetic portion was subtracted from the initial 0.15 grams before a percentage was determined. Figure 9

shows an example of a sample before and after the HCl step. The color in the second image is due to the less dense clay minerals that settle above the magnetic material in the HCl and rinsing processes.

Figure 9. Sample CP18 before HCl on the left and after HCl on the right.

Scanning Electron Microscope Analysis

Four samples were used for analysis using a scanning electron microscope (SEM). The samples used were CP0.2 from unit 1, CP18.0 from unit 3, CP31.5 and CP33.0 from unit 8. A portion of the magnetic material from before and after HCl treatment for each sample was mounted in a 1” round epoxy mount. Figure 10 shows the mount for two of the samples. The epoxy mounts were polished with1 μm diamond colloid to ensure grains were exposed and smooth, then the mount was coated with carbon.

Figure 10. Grain mount in epoxy for samples CP0.2 and CP18.0 before coating in carbon.

An SEM works by creating an electron beam that interacts with the sample. As the electron beam hits the sample, the sample emits both x-rays and electrons (Nesse, 2012). Backscatter electrons (BSE), are electrons that are deflected by the sample's atoms and can be used to create a visual image. Materials with higher average atomic number will appear brighter when imaged with BSE. Figure 11 shows an example of one of the BSE images for sample CP0.02. The bright grains were identified as the magnetic grains because of the higher atomic number of iron in comparison to the other grains in the samples. The BSE images were used to determine which grains to analyze for chemical analysis.

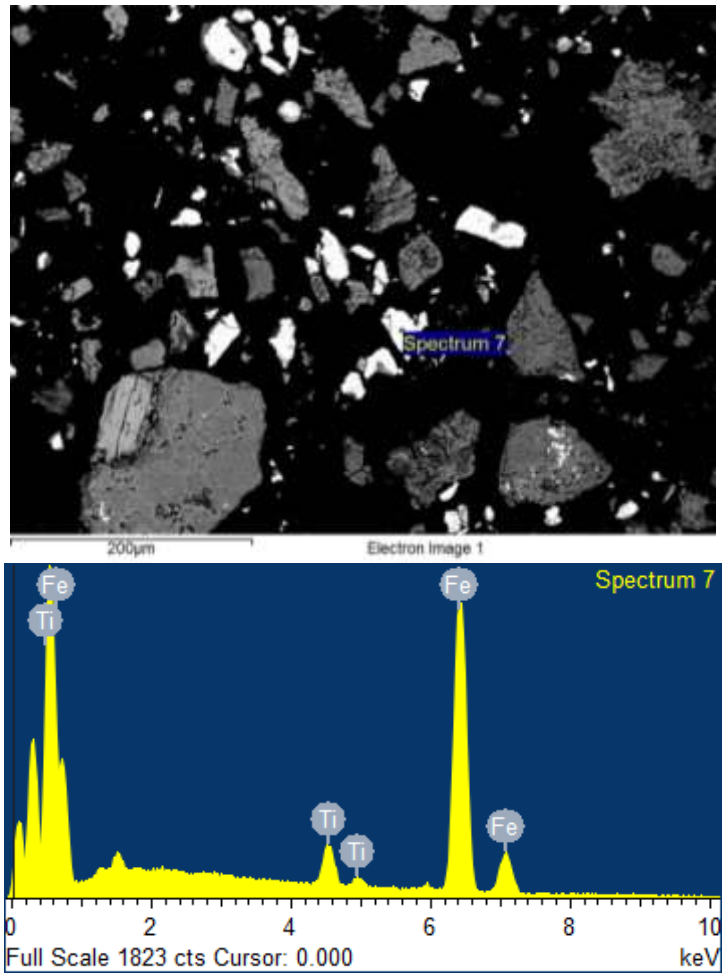

Figure 11. Top image is an example of a BSE image. The sample is from CP0.2 before HCl processing. The bottom is a X-ray spectrum of the spot indicated on the image.

For the chemical analysis, 25 bright grains from each sample were selected. The Energy Dispersive X-Ray Spectroscopy (EDS) determines the amount of x-rays at certain energies and presents that data as spectrum (Fig. 10 bottom). In an SEM, each element in volume that interacts with the beam electrons produces X-rays of specific energy that can be used to identify the presence of that element. Software calculates the weight percent of elements in this volume based on the amount of X-rays produced by a particular element.

Table 3 shows the weight percent results for spectrum 7 in Figure 10, oxygen is determined by charge balance, results are normalized to 100 total weight percent.

Table 3. Composition of Spectrum 7 CP0.2 before HCl processing

Element	Weight %
Ti	4.38
Fe	72.06
O	23.57
Total	100.00

The spectra were categorized based on weight percent of titanium. Samples with less than 15% were classified as low-titanium minerals. Samples with more than 15% were classified as high-titanium minerals. The weight percent of each element for all the grains in the group were averaged.

CHAPTER IV

RESULTS

Results of Magnetic Separation

Magnetic minerals make up only a small fraction of the composition of the rocks in the study area. The magnetic minerals made up less than 1% of the 300 g processed for each of the samples. The amount of magnetic minerals ranged from 0.05% to 0.63%. The data is shown in Table 4. The standard error for the average was also calculated.

Table 4. Results from magnetic separation. The average is the percent of the original 300 gram sample.

Unit	Sample	%Mag.	% Average	Standard Deviation	Standard Error
CPWL	CP55.5	0.26	0.22	0.07	0.04
	CP54.0	0.26			
	CP51.0	0.14			
12	CP48.0	0.27	0.27	0	0
	CP46.5	0.27			
11	CP45.0	0.2	0.24	0.04	0.02
	CP43.5	0.22			
	CP42.0	0.27			
	CP40.5	0.27			
10	CP39.0	0.3	0.315	0.02	0.04
	CP37.5	0.33			
9	CP36.0	0.19	0.19		
8	CP34.5	0.13	0.3	0.22	0.13
	CP33.0	0.25			
	CP31.5	0.63			
	CP30.0	0.2			

Table 4. Continued

Unit	Sample	%Mag.	% Average	Standard Deviation	Standard Error
6	CP28.5	0.45	0.45		
5	CP 27	No sample			
4	CP25.5	0.22	0.13	0.08	0.05
	CP24.0	0.09			
	CP22.5	0.08			
3	CP21.0	0.05	0.12	0.07	0.04
	CP19.5	0.11			
	CP18.0	0.19			
2	CP16.5	0.2	0.29	0.12	0.05
	CP15.0	0.37			
	CP13.5	0.24			
	CP12.0	0.41			
	CP9.0	0.46			
	CP7.5	0.15			
	CP6.0	0.2			
1	CP4.5	0.19	0.17	0.069	0.03
	CP3.0	0.14			
	CP1.5	0.1			
	CP0.2	0.26			

Results of the Hydrochloric Acid Process

The results from the HCl process are shown in Table 5. The values are percentages of the HCl sample which is the 0.15 g of magnetic mineral that was used for this step. T in this table indicates trace amounts (less than 0.01 g). The samples are organized in their relative position in the stratigraphic column. The majority of the samples had only trace amounts of magnetic minerals remaining after the HCl process, but 13 of the samples had measurable amounts. The amounts of remaining minerals ranged from 7.14% to 22.22%.

Table 5. Results of the HCl process. Data is shown as the percentage of the 0.15 g HCl sample.

Unit	Sample	Dissolved	Remaining	Average	Standard error
CPWL	CP55.5	100.00%	0	0.00	0.00
	CP54.0	100.00%	0		
	CP51.0	100.00%	0		
Unit 12	CP48.0	100.00%	0	0.00	0.00
	CP46.5	100.00%	0		
Unit 11	CP45.0	100.00%	0	0.00	0.00
	CP43.5	100.00%	0		
	CP42.0	100.00%	0		
	CP40.5	100.00%	0		
Unit 10	CP39.0	100.00%	0		0.00
	CP37.5	100.00%	0		
Unit 9	CP36.0	100.00%	0	0.00	0.00
Unit 8	CP34.5	100.00%	0	1.92	2.22
	CP33.0	100.00%	0		
	CP31.5	92.31%	7.69		
	CP30.0	100.00%	0		
Unit 6	CP28.5	100.00%	0	0.00	0.00
Unit 5	CP27.0	No sample	No sample		
Unit 4	CP25.5	90.91%	9.09	11.87	3.16
	CP24.0	91.67%	8.33		
	CP22.5	81.82%	18.18		
Unit 3	CP21.0	90.00%	10	9.39	5.26
	CP19.5	100.00%	0		
	CP18.0	81.82%	18.18		
Unit 2	CP16.5	87.50%	12.5	10.34	2.53
	CP15.0	88.89%	11.11		
	CP13.5	100.00%	0		
	CP12.0	88.89%	11.11		
	CP9.0	91.67%	8.33		
	CP7.5	92.86%	7.14		
	CP6.0	77.78%	22.22		
	CP3.0	90.91%	9.09		

Table 5 continued.

Unit	Sample	Dissolved	Remaining	Average	Standard error
Unit 1	CP4.5	100.00%	0	2.27	2.27
	CP3.0	90.91%	9.09		
	CP1.5	100.00%	0		
	CP.2	100.00%	0		

Results of Scanning Electron Microscope Analysis

The magnetic materials before and after the HCl process for four rock samples were analyzed using a scanning electron microscope. Appendix A contains the complete results of the SEM analysis. The mineral grains were sorted into in two groups. Grains that contained 15% or more of titanium belong to the high-titanium group and grains with less than 15% titanium belong to the low-titanium group. The average composition of weight percent for the low-titanium group is 69.04% FeO and 6.03% TiO_2. The values of the individual grains range from 60.10% FeO with 13.60% TiO_2 to 77% FeO and 0% TiO_2. The average composition of weight percent for the high-titanium group is 47.92% FeO and 23.98% TiO_2. The individual grains range from 35.98 FeO and 32.20% TiO_2 to 47.62% FeO and 15.34% TiO_2. Table 6 shows the averages for each of the samples before the HCl step. Table 7 shows the averages after the HCl step.

Table 6. Weight percent averages before HCl.

Sample	Low-titanium group		High-titanium group	
	FeO	TiO_2	FeO	TiO_2
CP 0.2	72.22	4.59	50.12	21.29
CP 18.0	70.05	3.38	42.49	27.19
CP 31.5	70.33	5.47	52.35	19.58
CP 33.0	70.26	5.21	47.62	23.22

Table 7. Weight percent averages after HCl.

Sample	Low-titanium group		High-titanium group	
	FeO	TiO_2	FeO	TiO_2
CP 0.2			49.95	24.02
CP 18.0	70.95	3.51	47.39	23.40
CP 31.5	61.92	12.19	44.72	24.88
CP 33.0	67.53	7.87	48.79	22.98

CHAPTER V

DISCUSSION AND CONCLUSIONS

Discussion of Magnetic Separation

The quantities of magnetic minerals are not consistent within lithographic units. The data for the magnetic separation is represented as a bar graph in Figure 12. Unit 2 has the greatest thickness of all the units had has the greatest number of samples. The seven samples are CP 6.0 to CP 16.5. The amount of magnetic minerals varies from 0.15% in sample CP 7.5 to 0.46% in the next sample CP 9.0. CP 12.0 also has a high value of 0.41% and CP 15.0 has 0.37%. The rest of the samples in this unit have amounts lower than 0.24%. There is variability within the unit has no a clear pattern.

There are two units that have four samples. In unit 1, the values for the percent of magnetic minerals starts at the base CP 0.2 with 0.26%, then drops to 0.10%, then increases in the next two samples to 0.14% then 0.19%. In unit 11 in the upper part of the stratigraphic column, the first two samples, CP 40.5 and CP 42 have 0.27% magnetic minerals then there is a decrease with the next samples having 0.22% and then 0.20%. Each of these examples indicate that even within the lithographic units, there can be variations in the amount of magnetic minerals.

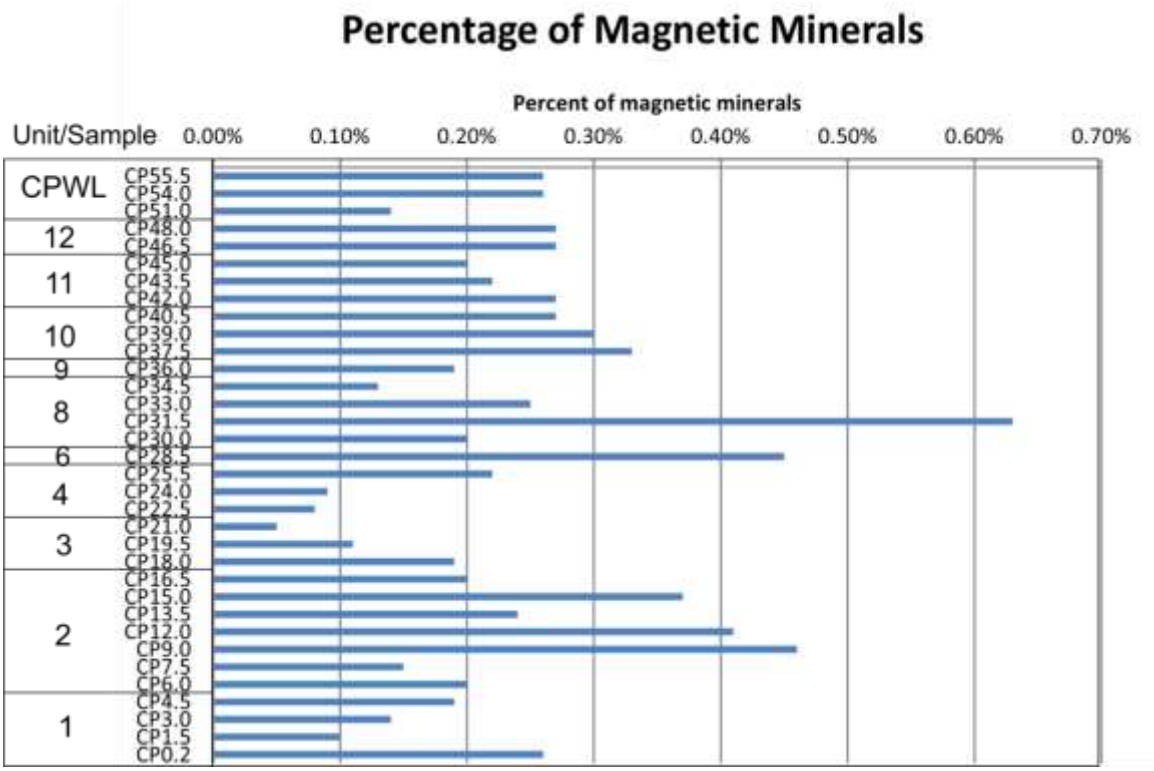

Figure 12. Results of the magnetic material separation as a percentage of the original 300 g sample. The rock samples are arranged by stratigraphic position.

There is also not a significant pattern of change in the percent of magnetic minerals at the unit boundaries. The average change between the percent of magnetic minerals at unit boundaries is 0.12% with the values ranging from 0.46% to 0.01%. The amount of change at unit boundaries is well within the fluctuation within individual units. In Figure 12, there are not clear changes that would represent a change from one unit to another.

There are slight variations in the quantity of magnetic minerals in different lithologies of rock. Based on the average, the sandstone in the study contained 0.265% magnetic minerals, siltstone was 0.19% and the single mudstone layer contained 0.13%. Looking at the individual samples, this pattern is not consistent. The sandstone samples ranged from 0.15% to 0.46%. The siltstone samples ranged from 0.1% to 0.63%.

Discussion of the Hydrochloric Acid Process

The HCl process uses a low-tech method to quantify the amount of magnetite in comparison to other magnetic minerals. HCl has been used in other studies to separate magnetic minerals (Gehring and others, 2007; Goulart and others, 1994). One of the major limitations is that this process cannot be used to confidently identify the specific minerals. Magnetite and hematite will both dissolve in HCl (Sidhu and others, 1981). Iron oxide minerals that contain titanium are more resistant to HCl dissolution (Gehring and others, 2007). At this point in the study, the designations of dissolved minerals will represent the minerals that dissolve in the HCl and HCl resistant minerals will represent the magnetic minerals that remained after the process. Figure 13 contains the results of the HCl process showing the HCl resistant magnetic minerals.

The majority of the magnetic minerals in each of the samples dissolved in HCl. The amount of dissolved minerals ranged from 77-100%. Only 13 of the 34 samples contained more than trace amounts of HCl resistant minerals. The presence of HCl resistant minerals is independent of lithology. Unit 2 and 11 are the two sandstone units. Unit 2 contains HCl resistant magnetic minerals and Unit 11 does not. Within unit 2, the majority of the samples contained HCl resistant minerals but CP 13.5 did not.

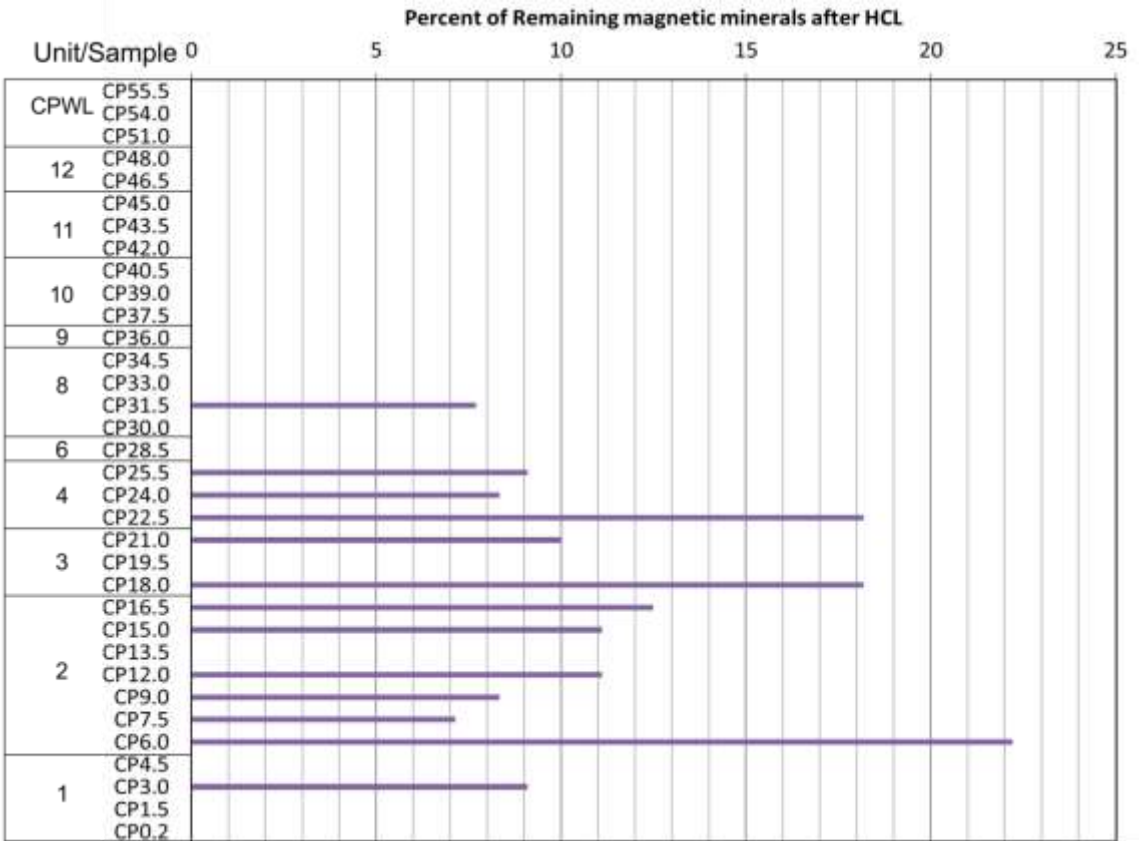

Figure 13.The percent of magnetic minerals for samples after the HCl process.

The most significant observation is that there are no HCl resistant minerals above CP31.5. In the lower section of the stratigraphic column, there are no clear patterns in the quantities of these minerals. The quantities range from 22.22% HCl resistant minerals to several samples with only trace amounts. The data also does not suggest a specific mechanism that could control these quantities.

It is possible that this change might be an indicator of a different source material for the sediment that formed the rocks. Larson and Evanoff (1998) studied the possible source area for volcanic tuffs in the White River sequence. They suggest that there was a change from rhyolitic to dacitic source volcanism. There are no tuffs in the lower Poleslide but it might suggest that erosional or transported materials could have come from another source. The magnetics alone are not sufficient evidence but it might be

beneficial to look at the other minerals present in these samples. It is also interesting that this change in the magnetic mineralogy in this section occurs in the middle of a unit without a significant change in lithology.

Other changes also occur at this section of the stratigraphic column that are significant. Unit 8 is the first unit where *Letyauchenia* fossils are abundant. This is one of the fossil assemblages that mark the division between the Orellan and Whitneyan land mammal ages (Benton and others, 2015). If this pattern is present at other locations, it might indicate that there is a mineral marker that could help in identifying this time marker in areas where fossils are not present.

This location also marks a transition between a normal polarity zone and a reversed polarity zone. While polarity is not going to affect the magnetic mineralogy present in the rock, it might be possible to use this magnetic change as a marker for this particular reversal. This might be helpful in correlating the polarity in the lower Poleslide in the Badlands. It is also possible that this is only present in the rocks in this area. It would be necessary to study other outcrops to see if this pattern is consistent.

Figure 14 combines the results of both the magnetic separation and the HCl process. The HCl resistant minerals are represented as the percent of the total magnetic sample. There are no clear patterns between the two sets of data. There is less variability in the quantities of magnetic minerals in the samples above CP 31.5. This image also puts the quantities in perspective. In both data sets the quantities are very small portions of the original 300 gram sample.

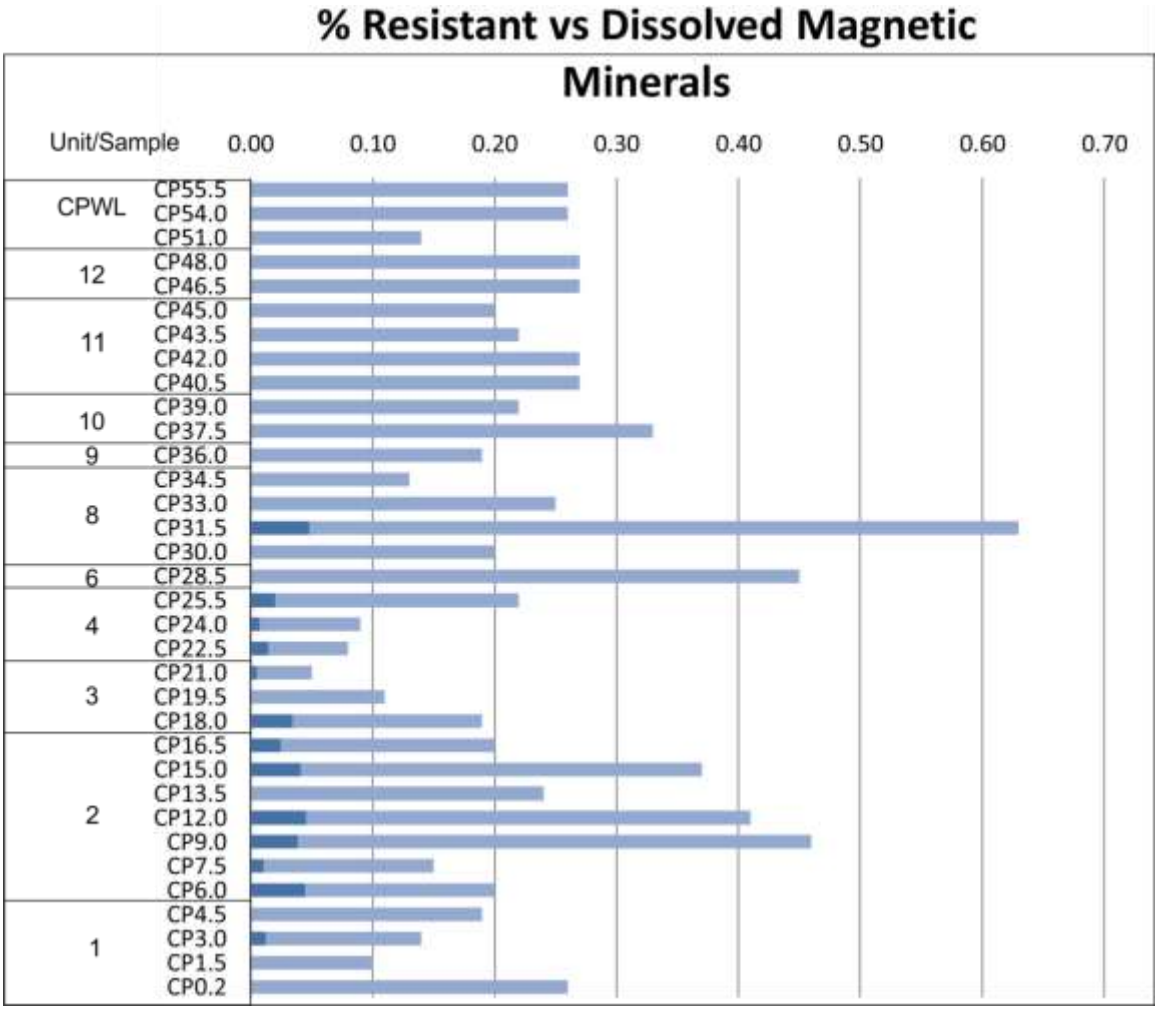

Figure 14. Combined results of the magnetic separation and HCl steps. The HCl resistant minerals are represented in dark blue as a percent of the magnetic sample.

Discussion of Scanning Electron Microscope Analysis

Prothero and others (1983) determined that the magnetic remanence carrier to be magnetite or titanomagnetite based on the paleomagnetic data. Magnetite is the most common magnetic mineral in rock with chemical formula of Fe_3O_4. It is one of the end members of a solid solution series with the other endmember being ulvöspinel $FeTiO_4$. There is a second solid solution series with end members of hematite FeO_3 and ilmenite $FeTiO_3$. A third series has end members of magnetite of Fe_3O_4 and ilmenite $FeTiO_3$.

Figure 15 shows a ternary diagram of these three solid solution series. Titanomagnetite refers to a mineral that falls between the endmembers of the magnetite – ilmenite solid solution series.

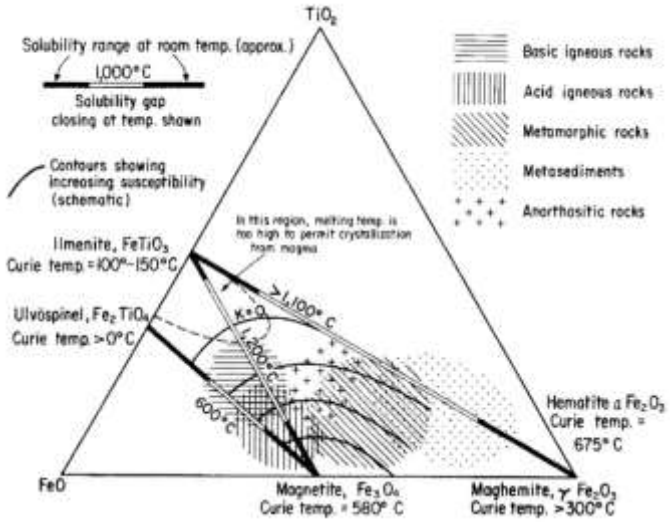

Figure 15. Ternary diagram showing the solid solutions series for magnetite, hematite, ilmenite, and ulvöspinel (Grant, 1984).

To determine the chemical formula of an analyzed magnetic mineral, the number of cations was calculated for four oxygen atoms for the magnetite-ulvöspinel series and for three oxygen atoms for the hematite-ilmenite series using the procedure described by Nesse (2012) using the average weight percentages. The closest match to the ideal formula determined the mineral.

In the four samples that were processed using the SEM, the most common mineral in the magnetic sample before processing was the low-titanium group. In each of the samples, the majority of the 25 grains that were analyzed were categorized in this group. The average composition for these minerals ranges from 100% FeO to 69.04% FeO and 6.03% TiO_2. Table 8 shows the number of cations calculated for the average composition.

Table 8. Calculated cations for the low titanium group

	Fe	Ti	Total
average weight.%	69.04	6.03	75.07
cations O_3	2.670	0.165	2.84
cations O_4	3.560	0.220	3.78

The calculated formula for the mineral to be hematite (Fe_2O_3) is $Fe_{2.84}O_3$ and for magnetite (Fe_3O_4) is $Fe_{3.78}O_4$. In both cases, the number of calculated cations for iron is high. The low-titanium minerals in this group are either magnetite or hematite but it is not possible to distinguish between the two using the SEM data. Based on the color change when HCl was added to the samples, this mineral would be magnetite. The calculated formula for ulvöspinel ($FeTiO_4$) is $Fe_{2.76}Ti_{0.619}O_4$ and for ilmenite ($FeTiO_{3)}$ is $Fe_{2.072}Ti_{0.319}O_3$. There is considerable variation between individual grains within this group and like the low-titanium group, the calculated cations do not fit cleanly into the chemical formulas for individual minerals.

The composition of the high-titanium minerals range from 53% FeO and 47% TiO_2 to 67% FeO and 33% TiO_2. The average composition for this group is 64% FeO and 36% TiO_2. Table 14 shows the calculated cations for the average composition. The calculated formula for ulvöspinel (Fe_2TiO_4) is $Fe_{2.012}Ti_{0.994}O_4$ and for ilmenite ($FeTiO_{3)}$ is $Fe_{1.509}Ti_{0.746}O_3$. In this case, the cations are correct for the formula for ulvöspinel. The values of the cations are closer to the formulas for the minerals, but there is still question to the actual measured quantities of the elements in the SEM results.

Table 9. Calculated cations for the high titanium group.

	Fe	Ti	Total
average weight.%	45.36	24.93	70.29
cations O_3	1.509	0.746	2.255
cations O_4		0.994	3.006

Two mineral standards that contain both iron and titanium were analyzed to determine the accuracy of the titanium and iron analyses. For kaersutite, the percent error between the EDS results and the standard for iron was 11% higher than the standard and for titanium 4% higher than the standard. For biotite, the percent error between the EDS data and the standard was 1% higher for iron and for titanium, 5% lower than the standard. Combining the variability in results with the likelihood of the minerals in the study falling between endmembers in the solid solution series, confident identification of individual minerals is not possible with this analysis technique.

Conclusions

There are two questions that this project was designed to answer.

Q1 What are the magnetic minerals and quantities of magnetic minerals in the Cedar Pass Section?

Q2 Are there any specific patterns in the distribution of magnetic minerals in the section?

Question 1

The exact minerology of the magnetic minerals in the Cedar Pass could not be determined by techniques used in this project. The quantities of magnetic minerals in the 300g samples that were processed ranged from 0.05% to 0.63%. This analysis showed that there were variations within stratigraphic layers that shared the same lithology but

not with a common pattern. There was also not a common pattern at the boundaries of layers. The small quantities of magnetic minerals also create a challenge. Any error or inconsistency in the separation process could affect the results.

The HCl process was used to separate magnetite from the more resistant titano-hematite or hemo-ilmenite. In this analysis, the amount of resistant magnetic minerals in the 0.15g samples ranged from 0 to 22.22%. There wasn't a clear pattern linked to lithology or location within a unit. The HCl process alone is not sufficient to determine the specific mineralogy of the section. The SEM analysis was not sufficient to identify the specific minerals and only 4 samples were tested. The grains sampled varied in the amounts of titanium present placing them between the end members in the solid solution for these minerals. For a complete analysis of the specific mineralogy, another technique such as microprobe analysis would be needed.

Question 2

There was variability in the quantities of magnetic minerals but not specific patterns. There are not any identifiable patterns within lithologies or clear changes at boundaries between units. There wasn't a significant increase or decrease in quantities of magnetic minerals moving up through the stratigraphic column. The most significant observation was the decrease to trace amounts of HCl resistant minerals above 33.0 m. CP 33.0 was the only sample of the rocks above this break that was analyzed with the SEM. The magnetic minerals were similar to the other samples analyzed but this sample may not represent the rest of the rocks in the section. The loss of acid resistant magnetic minerals represents a change in source mineralogy that may be a stratigraphic marker.

Future Research

One of the most important projects that could be done in this research is a complete microprobe analysis of all of the rock samples in this stratigraphic column. The use of a microprobe, would make a more confident identification of the minerals possible. This analysis would provide a clearer understanding of the specific magnetic minerology of the section. This would also answer any questions about a change in the magnetic minerology in the upper part of the column. This research might also make it possible to determine more specifically the mineralization of the magnetic minerals that are resistant to HCl.

The stratigraphic units of the lower Poleslide Member of the Brule Formation can be easily identified in other areas. It would be helpful to analyze this same member in a different location and compare the results. This research would indicate if the magnetic mineralogy was consistent in other locations. It would also be important to determine if the pattern of only trace amounts of HCl resistant magnetic minerals is a characteristic of the upper units of the member or are unique to this location.

REFERENCES CITED

Benton, R.C., Terry, D.O., Evanoff, E., and McDonald, H. G., 2015, The White River Badlands: Bloomington, Indiana, Indiana University Press, 196 p.

Benton, R.C., Evanoff, E.E., Herbel, C. L., and Terry Jr., D. O., 2009, Documentation of significant paleontological localities within the Poleslide Member, Brule Formation, Badlands National Park, South Dakota: National Resources Preservation Program Grant Final Report, on file at Badlands National Park, p. 69.

Clark, J., 1954, Geographic designation of the members of the Chadron Formation in South Dakota: Carnegie Museum Annals, v. 25, p. 197-198.

Evans, J.E., and Terry, D.O., 1994, The significance of incision and fluvial sedimentation in the basal White River Group (Eocene-Oligocene), Badlands of South Dakota, U.S.A., Sedimentary Geology, v.90, p. 137-152.

Evanoff, E., Terry Jr., D.O., Benton, R.C., and Minkler, H., 2010, Field guide to geology of the White River Group in the North Unit of Badlands National Park, South Dakota: School of Mines and Technology Bulletin 21, p.96-127.

Gehring, A.U., Fischer, H., Schill, J., Graneher, J., and Luster, J., 2007, The dynamics of magnetic ordering in a natural hemo-immenite solid solution: Geophysical Journal International, v. 169, i. 3, p. 917-925.

Goulart, A.T., de Jesus Filho, M. F., Fabris, J.D., and Coey, J.M.D., 1994, Characterization of a soil ilmentite developed from basalt: Hyperfine Interactions, v. 91 i. 1, p.771-6775.

Grant, F.S., 1984, Aeromagnetics, Geology and ore Environments, I. magnetite in igneous, sedimentary, and metamorphic rocks: an overview: Geoexloration, v. 23 p.303-333.

Larson, E.E., and Evanoff, E.E., 1998, Tephrostratigraphy and source of the tuffs of the White River sequence: Geologic Society of America Special Paper 325, p.1-14.

Nesse, W.D., 2012, Introduction to Mineralogy, second edition: New York, Oxford University Press, 496 p.

Osborn, H. F., and Matthew, W.D., 1909, Cenozoic mammal horizons of western North America: U.S. Geological Survey Bulletin 361, 138p.

Prothero, D.R., 1985, Correlation of the White River Group by magnetostratigrapy, In Martin, J.E., Fossiliferous Cenozoic deposits of western South Dakota and northwestern Nebraska: Dakoterra, Museum of Geology, South Dakota School Mines v. 2, p.265-276.

Prothero D.R., Denham, C.R., and Farmer, H.G, 1983, Magnetostratigraphy of the White River Group and its implications for Oligocene geochronology: Paleogeography, Paleoclimatology, Paleoecology, v.42. p.151-166.

Prothero, D.R., and Emery, R.J., 2004, The Chadronian, Orellan, and Whitneyan North American land mammal ages, in Woodburne, M.O., ed, Late Cretaceous and Cenozoic mammals in North America: New York, Columbia University Press, p.156-168.

Prothero, D.R., and Whittlesey, K.E., 1998, Magnetic stratigraphy and biostratigraphy of the Orellan and Whitneyan land-mammal "ages" in the White River Group, in Terry Jr, D.O., LaGarry, H.E., and Hunt Jr., R.M.,eds, Depositional environments, lithology, and biostratigraphy of the White River and Arikaree Groups (Late Eocene to Early Miocene, North America): Geological Society of America Special Paper 325, p39-61.

Prout, H.A., 1846, Gigantic *Palaeotherium*: American Journal of Science, v. 2, p.88-89.

Sidhu, P.S., Gilkes, R.J., Cornell, R.M., Posner, A.M., and Quirk, J.P., 1981, Dissolution of iron oxides and oxyhydroxides in hydrochloric and perchloric acids: Clay and clay minerals, v. 29, n. 4, p.269-276.

Stoffer, P.W., 2003, Geology of Badlands National Park: a preliminary report: U.S. Geological Survey Open-File Report 03-35-A, 63 p.

Tarling, D. H., 1999, Introduction: sediments and diagenesis, In Tarling, D.H., & Turner, P., Paleomagnetism and diagenesis in sediments: Geological Society, London, Special Publications, p. 151.

Tedford, R.H., Swinehart, J., Prothero, D.R., Swisher III, C.C., King, S.A., and Tierney, T.E., 1996, The Whitneyan-Arikareean tranition in the high planes; in Prothero, D.R., and Emery R.J., The terrestrial Eocene-Oligocene transition in North America: Cambridge, Cambridge University Press, p.312-334.

Wanless, H. R., 1923, Stratigraphy of the White River beds of South Dakota: American philosophical society proceedings, v. 62, p.190-269.

Wood, H.E., Chaney Jr., R.W., Clark, J., Colbert, E.H., Jepsen, G.L., Reeside Jr., J.B., and Stock, C., 1941, Nomenclature and correlation of the North American continental Tertiary: Geological Society of America Bulletin 52, p.1-48.

APPENDIX A

SCANNING ELECTRON MICROSCOPE RESULTS

Table 10. Weight percent results for CP 0.2 magnetic sample

		Low		High	
Spectrum		Fe	Ti	Fe	Ti
1		75.12	2.01		
2		70.09	5.89		
3		72.13	2.61		
4		74.9	2.18		
5		72.69	3.89		
6		72.89	3.74		
7		72.06	4.38		
8		72.27	4.21		
9		73.59	3.19		
10		77.73			
11		75.26	1.89		
12		67.35	8.01		
13		68.16	7.38		
14				45.78	24.64
15		71.97	4.45		
16		68.6	7.04		
17		70.12	5.87		
18		67.44	7.94		
19		77.73			
20		68.81	6.88		
21		73.06	3.60		
22				48.22	22.76
23		70.11	5.88		
24				56.35	16.49
25		76.76	0.75		
Average		72.22	4.59	50.12	21.29
Cations	O_3	2.691	0.154	1.701	0.650
	O_4	3.588	0.206	2.268	0.866

Table 11. Weight percent for CP 0.2 HCl sample

		Low		High	
Spectrum		Fe	Ti	Fe	Ti
1				46.25	24.28
2				51.57	20.18
3				44.35	25.75
4				45.34	24.98
5				51.38	20.33
6				51.20	20.47
7				45.96	24.51
8				45.56	24.81
9				46.13	24.37
10				46.52	24.07
11				45.73	24.68
12				45.63	24.76
13				46.27	24.27
14				43.65	26.28
15				51.32	20.37
16				45.25	25.06
17				45.66	24.58
18				45.86	24.58
19				48.70	22.39
20				46.22	24.30
21				45.89	24.56
22				46.10	24.39
23				52.20	19.70
24				42.46	27.20
25				48.65	22.43
Average				46.95	24.02
Cations	O_3			1.563	0.719
	O_4			2.083	0.958

Table 12. Weight percent for CP 18.0 magnetic sample

		Low		High	
Spectrum		Fe	Ti	Fe	Ti
1		67.60	7.81		
2		65.20	9.66		
3		61.22	12.22		
4		72.91	3.72		
5		69.65	6.24		
6		74.44	2.54		
7		72.06	4.37		
8		71.71	4.65		
9		73.52	3.25		
10		67.46	9.91		
11		71.60	4.73		
12				39.22	29.71
13		75.85	1.45		
14				45.76	24.66
15		67.46	7.92		
16		73.17	3.52		
17		63.60	10.90		
18		75.62	1.63		
19		71.62	4.72		
20		68.12	7.41		
21		71.34	5.01		
22		73.63	3.17		
23		76.31	1.10		
24		66.03	9.02		
25		61.03	12.88		
Average		70.05	3.38	42.49	27.19
Cations	O_3	2.760	0.120	1.395	0.803
	O_4	3.681	0.160	1.860	1.070

Table 13. Weight percent for CP 18.0 HCl Sample

		Low		High	
Spectrum		Fe	Ti	Fe	Ti
1				43.94	26.06
2				47.31	23.46
3				43.21	26.62
4		61.83	12.27		
5				50.56	20.94
6				48.18	22.79
7				49.13	22.06
8		74.81	2.25		
9				53.07	19.02
10				51.90	19.92
11				46.59	24.02
12				39.59	29.42
13				47.45	23.38
14				43.06	26.74
15				50.97	20.64
16				36.93	31.47
17		71.90	4.5		
18				48.17	22.80
19		74.28	2.81		
20				51.65	20.12
21				44.12	25.93
22				45.38	24.95
23				43.80	26.17
24				56.18	16.62
25				53.91	18.37
26		71.95	4.46		
Average		70.95	3.51	47.39	23.40
Cations	O_3	2.755	0.123	1.589	0.705
	O_4	3.673	0.163	2.119	0.967

Table 14. Weight percent for CP 31.5 Magnetic sample

		Low		High	
Spectrum		Fe	Ti	Fe	Ti
1		65.27	9.61		
2		72.72	3.87		
3		70.49	5.59		
4		69.31	6.49		
5		72.48	4.05		
6		72.49	4.04		
7		69.64	6.24		
8		67.25	8.08		
9		64.54	10.17		
10		71.80	4.57		
11				54.70	17.76
12		67.44	7.94		
13		77.42	0.24		
14		72.25	4.23		
15		70.02	5.94		
16		72.26	4.22		
17		69.05	6.70		
18		70.40	5.66		
19		70.23	5.79		
20		72.14	4.31		
21		70.82	5.25		
22				45.85	24.59
23		69.93	6.01		
24				56.49	16.38
25		69.26	6.53		
Average		70.33	5.47	52.35	19.58
Cations	O_3	2.632	0.184	1.794	0.603
	O_4	3.509	0.245	2.392	0.804

Table 15. Data for CP 31.5 HCl sample

		Low		High	
Spectrum		Fe	Ti	Fe	Ti
1				41.32	28.09
2					
3				43.54	26.37
4		61.92	12.19		
5				48.03	22.91
6				47.39	23.40
7				46.19	24.33
8				50.89	20.70
9				43.40	26.48
10				47.72	23.15
11				49.89	21.48
12				45.29	25.02
13				40.25	28.91
14				47.17	23.57
15				41.73	27.76
16				35.98	32.20
17				42.43	27.23
18				46.60	24.01
19				46.71	23.93
20					
21				38.91	29.94
22				45.71	24.70
23				44.59	25.56
24					
25				45.47	24.88
Average		61.92	12.19	44.72	24.88
Cations	O_3	2.216	0.392	1.5	0.750
	O_4	2.954	0.523	2.00	1.00

Table 16. Weight percent for CP 33.0 Magnetic Sample

		Low		High	
Spectrum		Fe	Ti	Fe	Ti
1		69.97	5.99		
2		69.64	6.24		
3		72.84	3.77		
4		71.80	4.58		
5		65.02	9.8		
6		75.35	1.83		
7				47.62	23.22
8		69.24	6.55		
9		76.14	1.23		
10		62.68	11.61		
11		68.51	7.11		
12		74.85	2.22		
13		65.87	9.15		
14		68.77	6.91		
15		67.88	7.60		
16		64.14	10.48		
17		76.95	0.60		
18		67.61	7.81		
19		70.44	5.62		
20		72.43	4.09		
21		70.16	5.84		
22		73.93	2.93		
23		72.43	4.09		
24		70.99	5.20		
25		68.75	6.92		
26		68.94	9.86		
27		64.21	10.43		
28		77.46	0.21		
Average		70.26	5.21	47.62	23.22
Cations	O_3	2.647	0.176	1.598	0.701
	O_4	3.529	0.235	2.131	0.934

Table 17. Weight percent for CP 33.0 HCl sample

		Low		High	
Spectrum		Fe	Ti	Fe	Ti
1				47.30	23.47
2				50.05	21.35
3				67.47	32.53
4				50.98	20.63
5				46.33	24.22
6				46.70	23.93
7				48.00	22.93
8				48.59	22.47
9				47.79	23.10
10				47.65	23.20
11				42.27	27.18
12		60.10	13.60		
13				41.85	27.67
14				47.62	15.34
15					
16					
17				42.17	27.43
18		64.63	10.1		
19				53.60	16.61
20				51.60	20.15
21		72.94	3.69		
22				53.03	19.05
23				51.73	20.06
24		72.45	4.07		
25				48.42	22.61
26				46.29	24.25
27				48.01	22.93
28				45.91	24.54
Average.		67.53	7.87	48.79	22.98
Cations	O_3	2.480	0.260	1.624	0.688
	O_4	3.307	0.347	2.166	0.917